p21 mediates macrophage reprogramming through regulation of p50-p50 NF-κB and IFN-β

Gorjana Rackov,[1] Enrique Hernández-Jiménez,[2] Rahman Shokri,[1] Lorena Carmona-Rodríguez,[1] Santos Mañes,[1] Melchor Álvarez-Mon,[3] Eduardo López-Collazo,[2] Carlos Martínez-A,[1] and Dimitrios Balomenos[1]

[1]Department of Immunology and Oncology, Centro Nacional de Biotecnología/Consejo Superior de Investigaciones Científicas (CNB-CSIC), Madrid, Spain. [2]Innate Immunity Group, IdiPAZ, La Paz Hospital, Madrid, Spain. [3]Immune System Diseases-Rheumatology and Oncology Service, University Hospital Príncipe de Asturias, Alcalá de Henares, Madrid, Spain.

M1 and M2 macrophage phenotypes, which mediate proinflammatory and antiinflammatory functions, respectively, represent the extremes of immunoregulatory plasticity in the macrophage population. This plasticity can also result in intermediate macrophage states that support a balance between these opposing functions. In sepsis, M1 macrophages can compensate for hyperinflammation by acquiring an M2-like immunosuppressed status that increases the risk of secondary infection and death. The M1 to M2 macrophage reprogramming that develops during LPS tolerance resembles the pathological antiinflammatory response to sepsis. Here, we determined that p21 regulates macrophage reprogramming by shifting the balance between active p65-p50 and inhibitory p50-p50 NF-κB pathways. p21 deficiency reduced the DNA-binding affinity of the p50-p50 homodimer in LPS-primed and -rechallenged macrophages, impairing their ability to attenuate IFN-β production and acquire an M2-like hyporesponsive status. High p21 levels in sepsis patients correlated with low IFN-β expression, and p21 knockdown in human monocytes corroborated its role in IFN-β regulation. The data demonstrate that p21 adjusts the equilibrium between p65-p50 and p50-p50 NF-κB pathways to mediate macrophage plasticity in LPS tolerance. Identifying p21-related pathways involved in monocyte reprogramming may lead to potential targets for sepsis treatment.

Introduction

Monocytes and macrophages play key functions in defense against pathogens and activation of adaptive immunity, as well as in initiation and resolution of inflammation (1, 2). One extraordinary property of macrophages that has been studied in recent years is their plasticity. M1 (classically activated or proinflammatory) and M2 (alternatively activated or antiinflammatory) represent extremes of macrophage polarization (3–6). Macrophage plasticity includes intermediate states, some of which are termed M2a, Mb, and M2c (7, 8). M1 macrophages produce proinflammatory cytokines and eliminate intracellular microorganisms and tumor cells (9). Alternatively, M2 macrophages are involved in resolution of inflammation, parasite clearance, and allergic lung inflammation (9), and are identified as resident macrophages (6, 10). Macrophage plasticity maintains balance between M1 and M2 forms, as loss of optimal representation and/or appropriate recruitment can lead to harmful imbalance.

Microbial LPS and IFN-γ polarize macrophages to M1, while IL-4, IL-13, IL-10, TGF-β, glucocorticoids, and immune complexes give rise to M2 phenotypes (5, 11). M2 macrophages can also be generated after long or repeated exposure to LPS and are referred to as LPS- or endotoxin-tolerant macrophages (12, 13). These macrophages are hyporesponsive to subsequent LPS challenge and downregulate M1-associated proinflammatory mediators such as TNF-α, IFN-β, and iNOS (14, 15). LPS-tolerant macrophages upregulate prototypical M2 genes such as those encoding arginase I,

IL-10, and Th2-associated chemokines such as CCL2 (12, 16). These M2 cells might nonetheless have characteristics that render them distinct from typical M2 macrophages (13).

The refractory state of human monocytes after induction of endotoxin tolerance is also known as hyporesponsiveness or an immunosuppressive state, and a similar state of monocyte deregulation is observed in sepsis patients (17–19). Sepsis is a complex condition characterized by increased proinflammatory cytokines, caused by a decontrolled innate response following systemic bacterial infection (20). Inflammatory cells subsequently enter a state of hyporesponsiveness and become tolerant to further challenge. Monocytes isolated from sepsis patients thus produce low proinflammatory cytokine profiles when stimulated ex vivo with LPS (21). Monocyte hyporesponsiveness in sepsis is a reprogrammed state with alternative functional activity (17, 19, 21). Immunosuppression is considered a compensatory mechanism that regulates hyperinflammation to alleviate deleterious septic shock (22, 23). Nevertheless, this antiinflammatory response correlates with sepsis progression and death, and could increase the risk of secondary infection (20) or lead to influx of other inflammatory cells (18, 24). In mice, septic shock can be induced by a single LPS delivery, which corresponds to the initial proinflammatory response in sepsis. On the other hand, endotoxin tolerance induced by LPS priming and rechallenge drives macrophage immunosuppression (25, 26) and can be used to study hyporesponsiveness in sepsis (23).

The mechanism that regulates macrophage reprogramming from M1 to M2 during endotoxin tolerance remains undefined. Overexpression of certain negative regulators of the TLR4 pathway, including interleukin-1 receptor–associated kinase-M (IRAK-M), A20, and SH2-containing inositol-5′-phosphatase (SHIP), is associ-

ated with macrophage unresponsiveness (22, 27–29). The IRAK-M inducer hypoxia-inducible factor-1α (HIF1α) was also identified as a mediator of endotoxin tolerance (19). Moreover, accumulation of the p50 NF-κB subunit and predominance of p50-p50 over p65-p50 NF-κB levels is linked to macrophage hyporesponsivenes (30, 31). p50 lacks a transcription activation domain; when bound as a homodimer to gene promoters, it blocks binding of active p65-p50 NF-κB and thus inhibits gene expression (32, 33). Indeed, p50 deficiency leads to defective macrophage tolerance and M1 to M2 polarization (12). Although NF-κB regulation is a key event in orchestrating M1 versus M2 responses in LPS-tolerant macrophages, the mechanism that regulates this NF-κB–dependent plasticity remains undefined.

A characteristic of endotoxin tolerance is the downregulation of proinflammatory cytokines such as TNF-α and IFN-β (34). TNF-α regulation depends on NF-κB activation through TLR4 stimulation. Although diverse pathways are considered for IFN-β regulation (35, 36), its control is also linked to the NF-κB pathway and p50 regulatory activity (12). As IFN-β is essential during gram-negative bacterial infection in humans, a role for IFN-β in the pathology of sepsis was also proposed (37).

p21 is known primarily as a cyclin-dependent kinase 2 (CDK2) inhibitor (38). It is now established that, independently of this function, p21 is a central regulator of innate and adaptive immunity (39–43). p21 suppresses autoimmunity through T cell regulation (44), and we recently described a therapeutic effect for p21 through regulation of memory T cell responses and IFN-γ production in lupus-prone mice (45).

In addition to regulating T cell responses, p21 modulates innate immunity, as p21 deficiency increases LPS-induced NF-κB activation (46), proinflammatory cytokine production by macrophages, and septic shock (46–48). p21 also showed therapeutic value for macrophage regulation in a rheumatoid arthritis model (48). p21 thus negatively regulates the macrophage inflammatory response.

Here we analyzed the role of p21 in M2 macrophage polarization after LPS-induced tolerance in mice and in hyporesponsive monocytes from sepsis patients. We show that in the absence of p21, macrophage ability to develop in vivo tolerance was impaired in mice, leading to death. Furthermore, we found that p21 favors p50-p50 binding to NF-κB sites on DNA, which limits IFN-β production and allows M1 to M2 macrophage reprogramming. Our findings were complemented by data showing that monocytes from sepsis patients had high p21 levels that correlated with low IFN-β expression and a hyporesponsive phenotype. Overall, the data provide potentially new mechanistic insight into macrophage immunosuppression, and establish p21 as a key molecule in regulating the balance between inflammatory and hyporesponsive states.

Results

Requirement for p21 in LPS tolerance induction in mice. p21 is reported to be a regulator of inflammation, as its deficiency increases macrophage responsiveness and enhances the sensitivity of mice to LPS-induced septic shock (46). LPS tolerance and survival is manifested in mice after a robust LPS treatment, which is preceded by a sublethal LPS challenge (25, 26). As LPS tolerance is consistent with reduced inflammatory capacity of monocytes in sepsis

patients (21), we inquired whether p21 regulates induction of LPS tolerance through its antiinflammatory function.

To induce endotoxin tolerance in WT and *P21^{-/-}* mice in vivo, we administered a sublethal LPS dose, followed 16 hours later by a high LPS dose, and mice were monitored for 72 hours. Whereas a single lethal dose resulted in similar death induction in WT and *P21^{-/-}* mice (Figure 1A), we detected a significant difference in WT and *P21^{-/-}* mouse survival after induction of endotoxin tolerance (Figure 1A). The majority of WT mice achieved tolerance after secondary LPS challenge, while *P21^{-/-}* mice did not (~60% died by 24 hours after LPS challenge and 100% by 60 hours, Figure 1A). We also assessed proinflammatory cytokine profiles at 2 hours after the second LPS delivery, and found significantly increased serum TNF-α and IFN-β in *P21^{-/-}* compared with WT mice (Figure 1B). We thus hypothesized that p21 might be critical in regulating the reprogramming of M1 to M2 hyporesponsive macrophages.

p21 controls proinflammatory macrophage activity after in vivo induction of LPS tolerance. CD11b$^+$F4/80^{lo} small macrophages and CD11b$^+$F4/80^{hi} large macrophages (49–51) have been identified in the peritoneum. We tested whether lack of p21 affects these macrophage populations during in vivo induction of LPS tolerance. The relative proportions of peritoneal CD11b$^+$F4/80^{lo} and CD11b$^+$F4/80^{hi} cells were similar in WT and *P21^{-/-}* mice after dual PBS treatment, showing a preponderance of F4/80^{hi} with an approximately 10:90 ratio of F4/80^{lo}:F4/80^{hi} (Figure 2A). After dual LPS treatment, this ratio was approximately 50:50 in both WT and *P21^{-/-}* mice (Figure 2A). Absolute macrophage numbers were also similar in peritoneal exudates of WT and *P21^{-/-}* mice before and after dual LPS treatment (Figure 2A), suggesting no apparent p21 effect on the macrophage populations during LPS tolerance. However, analysis of the activation state of these populations showed a greater than 2-fold increase in TNF-α production in *P21^{-/-}* compared with WT F4/80^{lo} macrophages, indicating a very high M1-like macrophage response in the absence of p21 (Figure 2B). MHC class II and CD40 activation markers were also higher in *P21^{-/-}* compared with WT F4/80^{lo} macrophages (Supplemental Figure 1; supplemental material available online with this article; doi:10.1172/JCI83404DS1). In F4/80^{hi} macrophages, which produced low TNF-α levels, lack of p21 led to a significant increase in TNF-α production (Figure 2C). MHC class II and CD40 activation markers were highly expressed in WT macrophages (>80%) and did not increase further in *P21^{-/-}* F4/80^{hi} macrophages (Supplemental Figure 1). These data show that although lack of p21 does not change the relative proportions of peritoneal macrophage populations, it increases their activation and the M1 proinflammatory state.

To further examine the effect of p21 deficiency on macrophages in vivo, we analyzed splenic macrophages, which are also strongly affected by i.v. LPS challenge (52). As for peritoneum, we identified CD11b$^+$F4/80^{lo} and CD11b$^+$F4/80^{hi} splenic macrophage populations in both mouse strains, which changed in proportion following LPS+LPS treatment (Supplemental Figure 2). *P21^{-/-}* mice again showed proportions of the 2 populations as well as absolute macrophage numbers, similar to WT mice (Supplemental Figure 2). Nonetheless, expression of MHC class II and CD40 activation markers was clearly increased in p21-deficient CD11b$^+$F4/80^{lo} compared to WT macrophage subsets, which confirmed a broad-spectrum p21 effect on macrophage activity in endotoxin tolerance.
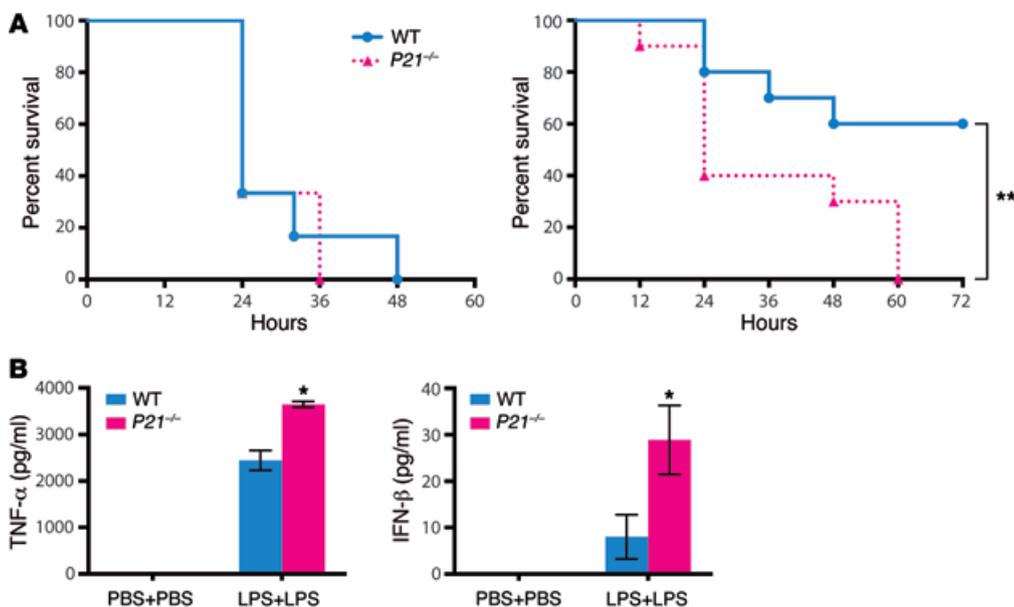
Figure 1. p21 controls in vivo endotoxin tolerance. (A) *P21⁻ᐟ⁻* and WT mice (*n* = 6) were treated with a single, high LPS dose, and showed 100% death (left). To induce tolerance, *P21⁻ᐟ⁻* and WT mice (*n* = 10) received a low LPS dose, followed by a high dose after 16 hours. *P21⁻ᐟ⁻* mice did not develop tolerance compared to WT mice, as indicated by a Kaplan-Meier survival curve (right). **$P < 0.01$, log-rank (Mantel-Cox) test. **(B)** Blood was collected 2 hours after the second LPS injection and serum cytokines measured by ELISA. Levels of M1-associated cytokines (TNF-α and IFN-β) were elevated in the serum of *P21⁻ᐟ⁻* compared with WT mice. Data show the mean ± SD (*n* = 3 mice), *$P < 0.05$, 2-tailed Student's *t* test.

phages were treated with LPS (20 hours), washed, allowed to rest (2 hours), and restimulated with LPS (4 hours) (ref. 12 and Figure 3A). This was followed by RT-PCR analysis of prototypical M1 and M2 gene expression in unstimulated, LPS-activated, and LPS-tolerized macrophages alone or with LPS restimulation. Whereas tolerant WT macrophages acquired an M2 polarization profile characterized by high expression of prototypic M2 genes (*Arg1*, *Ym1*, *Ccl17*), expression of these genes was defective in *P21⁻ᐟ⁻* macrophages (Figure 3B). Moreover, WT macrophages were tolerized, as reflected by downregulation of M1 genes (*Il1b*, *Tnfa*, *Ifnb*), whereas *P21⁻ᐟ⁻* macrophages did not develop tolerance and showed significantly higher M1-associated cytokine levels after LPS rechallenge (Figure 3C). These results revealed a critical role for p21 in M1 to M2 macrophage reprogramming. The finding that *Ifnb* mRNA was upregulated in tolerized *P21⁻ᐟ⁻* macrophages even without LPS restimulation (Figure 3C) suggests that p21 and IFN-β are closely linked in the regulation of M1 to M2 macrophage reprogramming.

P21⁻ᐟ⁻ macrophages secreted increased IFN-β levels even before LPS rechallenge (Figure 3D), which corroborated the RT-PCR data (Figure 3C). After LPS rechallenge, p21 deficiency caused a remarkable increase in TNF-α and IFN-β secretion and a significant reduction in the M2 chemokine CCL17 (Figure 3D), confirming a role for p21 in macrophage tolerization. Evaluation of IL-10 expression, which is upregulated during endotoxin tolerization and rechallenge (12), indicated impaired IL-10 induction in *P21⁻ᐟ⁻* macrophages (Supplemental Figure 4).

LPS activates endothelial cells and increases sepsis severity in mouse models (58). These cells also become tolerant after repeated LPS encounter (59). We examined whether p21 affected endotoxin tolerance of lung endothelial cells. We detected a significant mRNA increase in target molecules in *P21⁻ᐟ⁻* compared to WT cells after primary LPS stimulation, which included IFN-β (*P21⁻ᐟ⁻* vs. WT, $P < 0.001$) and TNF-α (*P21⁻ᐟ⁻* vs. WT, $P < 0.001$) (Supplemental Figure 5). This was accompanied by increased IFN-β protein production in *P21⁻ᐟ⁻* compared to WT cultures, although absolute protein levels were very low compared to IFN-β production by macrophages (Figure 3D). After LPS rechallenge, WT and *P21⁻ᐟ⁻* endothelial cells entered a tolerant state, as *Ifnb* mRNA and protein levels were greatly reduced. Similarly, *Tnfa* and *iNOS* reduction indicated *P21⁻ᐟ⁻* endothelial cell tolerization (Supplemental Figure 5), which implies that p21 deficiency does not affect endothelial LPS tolerization. p21 thus drives M1 to M2

As dendritic cells, and especially plasmacytoid dendritic cells (pDCs), respond to LPS by producing IFN-β (53, 54), we examined these cells in p21-deficient mice during LPS tolerance. After exclusion of CD19⁺ B cells, we identified CD11cʰⁱB220⁻ conventional dendritic cells (cDCs) and CD11cⁱⁿᵗB220⁺ pDCs (55) in spleen (Supplemental Figure 2). Both DC subsets upregulated MHC class II and CD69 activation markers following dual LPS challenge; however, this upregulation was similar in WT and *P21⁻ᐟ⁻* mice (Supplemental Figure 2), which suggested no p21 effect on these populations.

As both B and T lymphocytes are important in the pathophysiology of LPS-induced septic shock (56, 57), we analyzed the activation of these cells in WT and *P21⁻ᐟ⁻* mice during LPS tolerance. Although splenic CD19⁺ B cells upregulated MHC class II, CD86, and CD25 activation markers after dual LPS challenge, we observed no difference between WT and *P21⁻ᐟ⁻* cells (Supplemental Figure 3). As IFN-γ production and CD69 expression by T cells depend on p21 (45), we tested CD4⁺ and CD8⁺ T cells in WT and *P21⁻ᐟ⁻* mouse spleens and found similar IFN-γ production and CD69 upregulation (Supplemental Figure 3). The impaired in vivo LPS tolerization of *P21⁻ᐟ⁻* mice is thus mainly due to the increased proinflammatory state of *P21⁻ᐟ⁻* macrophages.

M1 to M2 macrophage polarization requires p21. Our in vivo results suggest that lack of p21 promotes M1 macrophage responses and interfere with M2 polarization during endotoxin tolerance. To examine this possibility, we studied the role of p21 in macrophage polarization during in vitro LPS tolerance. In macrophages, tolerance is induced by prolonged LPS treatment, which leads to acquisition of an M2 phenotype and reduced responsiveness of M1-associated genes after a second LPS challenge (12). To induce endotoxin tolerance in vitro, murine peritoneal macro-

Figure 2. p21 limits M1 activity during in vivo endotoxin tolerance. *P21⁻/⁻* and WT mice received 2 LPS doses as in Figure 1. (**A**) At 2 hours after the second LPS injection, macrophage populations from peritoneal exudates were analyzed by flow cytometry. Representative plots show gated CD11b^hi^F4/80^lo^ and CD11b^hi^F4/80^hi^ macrophages. The relative percentages of these 2 populations within the total F4/80⁺ gate, as well as total macrophage numbers, were similar for WT and *P21⁻/⁻* mice after dual LPS or PBS treatment (right). Data show the mean ± SD ($n = 8$); NS, not significant. (**B**) Intracellular staining showed that after dual LPS challenge, TNF-α production by F4/80^lo^ macrophages was higher in *P21⁻/⁻* compared with WT mice. Data show the mean ± SEM ($n = 4$); **$P < 0.01$. (**C**) After dual LPS treatment, intracellular TNF-α levels were elevated in *P21⁻/⁻* F4/80^hi^ compared with WT macrophages. Data show the mean ± SEM ($n = 4$ mice), *$P < 0.05$, 2-tailed Student's *t* test. SS, side scatter.

macrophage polarization and regulates IFN-β, a key cytokine in the control of this process.

p21 promotes macrophage tolerization by controlling IFN-β levels. The data suggest that p21 might promote macrophage polarization and hyporesponsiveness. Accordingly, LPS-tolerant and -rechallenged macrophages expressed high p21 levels (Figure 4A). p21 protein levels were also high in WT macrophages after LPS tolerization (time 0; Figure 4A) and after secondary LPS treatment (Figure 4A). p21 expression was also elevated after initial LPS activation (Figure 4A and Supplemental Figure 6), which corroborated previous findings (46). Lack of p21 affects macrophage activation in a cell cycle–independent manner (46). After LPS rechallenge, CDK2 phosphorylation activity, the major p21 target, was similarly low in *P21⁻/⁻* and WT macrophages (Supplemental Figure 8). Cell cycle analysis also showed both macrophage types in the G0/G1 stage after LPS rechallenge (Supplemental Figure 9). These data suggest that p21 deficiency impairs LPS tolerance without affecting CDK2 activity.

To confirm a cause/effect role for p21 in IFN-β regulation, we tested whether lack of p21 promotes IFN-β–dependent events such as STAT1 phosphorylation (pSTAT1) and expression of M1-associated genes (e.g., *Cxcl11* and *iNOS*) (36). After primary

LPS stimulation, pSTAT1 expression was similarly high in *P21⁻/⁻* and WT macrophages (Supplemental Figure 6). Following LPS tolerization, however, WT cells showed low pSTAT1 levels (time 0; Figure 4B), indicative of effective tolerization, while *P21⁻/⁻* macrophages exhibited high pSTAT1. After secondary LPS treatment, STAT1 phosphorylation remained considerably higher in p21-deficient than in WT macrophages at 15, 30, and 60 minutes (Figure 4B). The association of p21 with pSTAT1 regulation was further supported, since lack of p21 led to significantly higher iNOS and CXCL11 levels after secondary LPS activation (Figure 4C). These results suggest that p21 is critical for macrophage hyporesponsiveness induction by regulating IFN-β–dependent STAT1 activation. This view was reinforced by the elevated IFN-β production by *P21⁻/⁻* compared to WT macrophages, as shown earlier (Figure 3C).

To provide direct evidence that lack of p21 enhances IFN-β production and promotes STAT1 phosphorylation, we treated *P21⁻/⁻* macrophage cultures with an IFN-β–blocking antibody (or an isotype control). Antibody treatment lasted for the 20 hours of LPS tolerization, after which cells were washed and rechallenged with LPS. This treatment efficiently reduced STAT1 phosphorylation as well as iNOS protein levels in *P21⁻/⁻* cells, after tolerization (time 0; Figure 4D) and after secondary LPS treatment (Figure 4D). Simi-
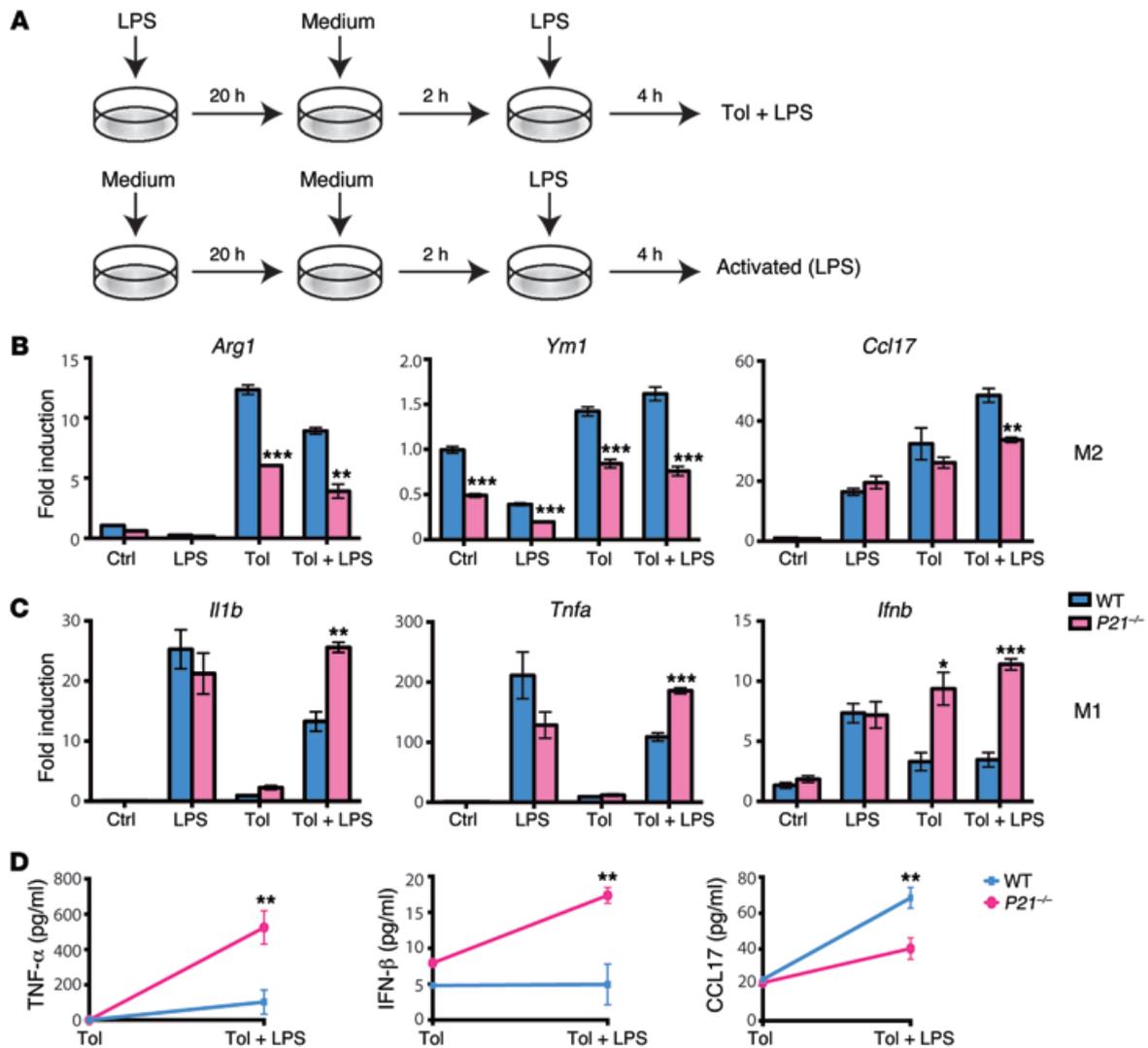
Figure 3. *P21⁻/⁻* macrophages show impaired ability to polarize to M2 cells during in vitro endotoxin tolerance. (**A**) Scheme showing the in vitro endotoxin tolerance model. Peritoneal macrophages from WT and *P21⁻/⁻* mice were tolerized with 100 ng/ml LPS for 20 hours (Tol), washed with PBS, cultured in medium (2 hours), and restimulated with 100 ng/ml LPS for 4 hours (Tol + LPS). LPS-activated cells were stimulated with LPS for 4 hours without previous tolerization (LPS). Cells left untreated were controls (Ctrl). Total RNA was extracted at 4 hours after LPS treatment and analyzed for gene expression. Culture supernatants were analyzed for cytokine production. (**B**) RT-PCR analysis showed impaired upregulation of M2-associated genes in *P21⁻/⁻* compared with WT macrophages after tolerization. (**C**) RT-PCR showed upregulation of representative M1 cytokine genes in *P21⁻/⁻* compared with WT tolerized macrophages. Results were normalized to β-actin and represent fold induction over unstimulated WT cells. (**D**) M1-associated TNF-α and IFN-β and M2-associated CCL17 production in WT and *P21⁻/⁻* macrophages at different time points after LPS restimulation, as measured by ELISA. In all cases data show the mean ± SEM (*n* = 3 independent experiments), *$P < 0.05$, **$P < 0.01$, ***$P < 0.001$, 2-tailed Student's *t* test.

larly, RT-PCR analysis showed a sharp drop in iNOS (>70%) and the M1-associated chemokine CXCL11 (>80%) (Figure 4E). TNF-α and endogenous IFN-β expression were unaffected by the blocking antibody treatment, showing that elevated IFN-β mostly affects the pSTAT1-dependent M1 characteristics. IFN-β blockade elicited M2-promoting adjustments and led to increased production of M2-associated CCL17 and CCL22 chemokines, which are key for LPS-induced macrophage tolerance (12), while arginase 1 was unaffected by the treatment (Figure 4E). The reduction in the *iNOS:Arg1* balance, an indicator of M1 to M2 skewing, suggests that IFN-β neutralization drives *P21⁻/⁻* macrophages towards an M2 phenotype. The data suggest that the inability of *P21⁻/⁻* macrophages to achieve a hyporesponsive state is directly associated with high IFN-β levels.

Treatment of *P21⁻/⁻* macrophage cultures with an anti–TNF-α blocking antibody had no major effects in reverting the M1 traits of *P21⁻/⁻* macrophages, as compared to IFN-β neutralization. Beyond moderate downregulation of iNOS production, compared to the massive iNOS downregulation after IFN-β neutralization, no other M1 or M2 features were affected (CXCL11 or CCL17, and CCL22 expression) (Figure 4E). STAT1 phosphorylation was mainly unaffected by TNF-α neutralization (Supplemental Figure 7). The data show that compared to TNF-α, IFN-β has a more relevant role in hindering M1 to M2 polarization of *P21⁻/⁻* macrophages.

To determine whether the effects of elevated IFN-β production by *P21⁻/⁻* macrophages extended beyond the 20-hour tolerization time frame, we initiated IFN-β neutralization after this
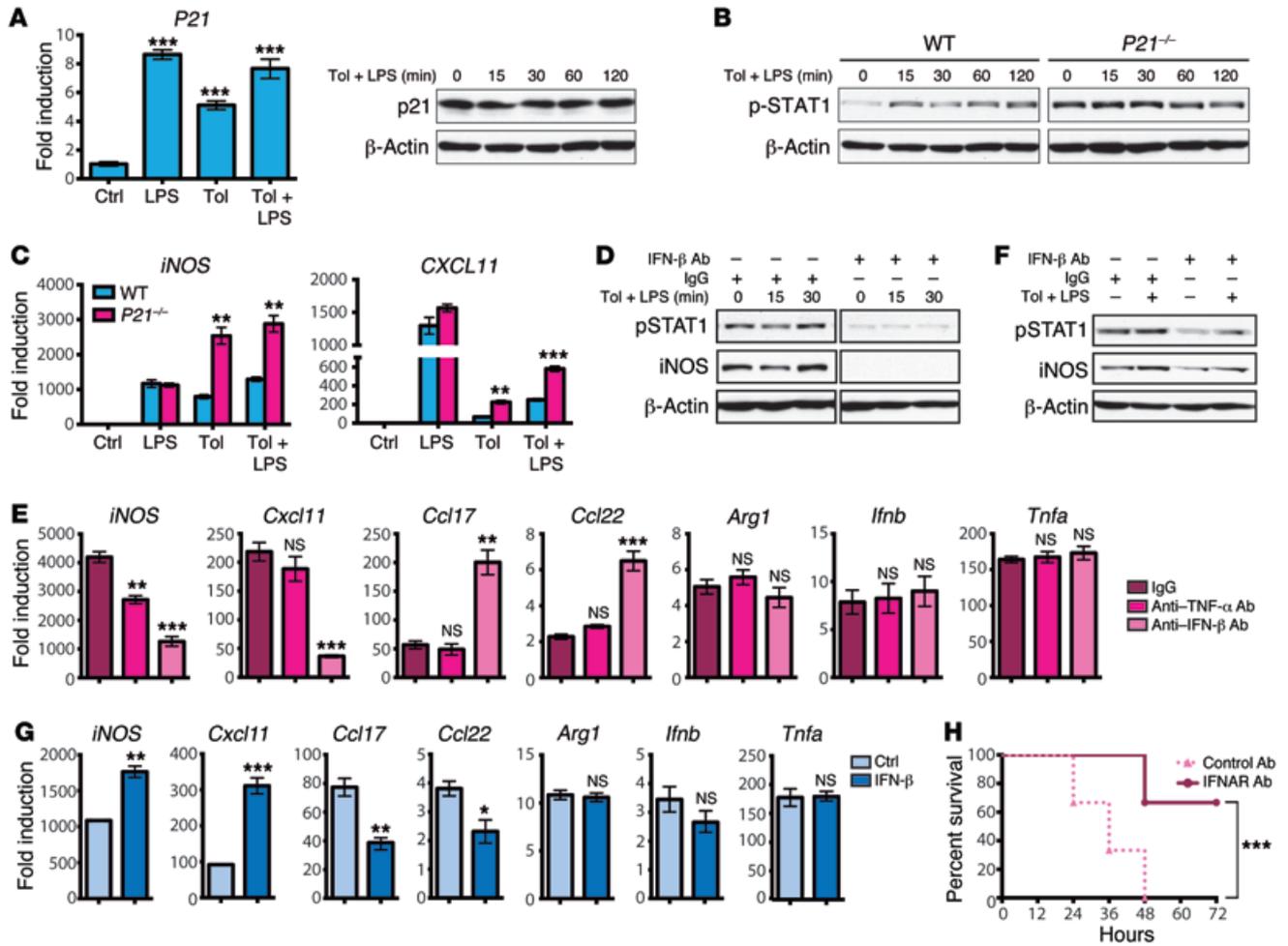
Figure 4. IFN-β neutralization reduces STAT1 phosphorylation and induces hyporesponsiveness in *P21*⁻/⁻ macrophages. (**A**) *P21* mRNA and protein levels in LPS-rechallenged WT macrophages. (**B**) STAT1 phosphorylation in WT and *P21*⁻/⁻ macrophages. (**C**) Increased iNOS and CXCL11 expression in tolerized *P21*⁻/⁻ macrophages. (**D** and **E**) *P21*⁻/⁻ peritoneal macrophages were incubated with an IFN-β– or TNF-α–neutralizing antibody or an isotype control during LPS tolerization (20 hours). Cells were washed, cultured in medium (2 hours) and restimulated with LPS (4 hours). (**D**) Reduction in STAT1 phosphorylation and iNOS expression after antibody treatment at indicated times. (**E**) RT-PCR analysis of *P21*⁻/⁻ macrophages incubated with appropriate antibodies during LPS tolerization (20 hours) and restimulated with LPS (4 hours). (**F**) After LPS tolerization, *P21*⁻/⁻ macrophages were restimulated with LPS (4 hours) in the presence of anti–IFN-β or isotype control antibody. Immunoblot shows a reduction in STAT1 phosphorylation and iNOS expression. (**G**) WT macrophages were treated with IFN-β during LPS tolerization, restimulated with LPS (4 hours), and analyzed by RT-PCR. (**H**) *P21*⁻/⁻ mice were challenged with 2 LPS doses as in Figure 1. At 2 hours before LPS rechallenge, mice were treated i.p. with anti-IFNAR1 antibody or control IgG. Inhibition of IFNAR1 improved tolerance to LPS, as shown by a Kaplan-Meier survival curve (*n* = 9), ***P < 0.001, log-rank (Mantel-Cox) test. For all RT-PCR analyses, results were normalized to β-actin and show fold induction over unstimulated WT cells. Data shown as the mean ± SEM (*n* = 3 independent experiments), *P < 0.05, **P < 0.01, ***P < 0.001. For **A** and **E**, 1-way ANOVA. For **C** and **G**, 2-tailed Student's *t* test. NS, not significant. For immunoblots, β-actin was used as a loading control. Western blots in **A** and **B** were derived from the same experiment. Representative gels of 3 experiments are shown.

process. p21-deficient macrophages were tolerized with LPS (20 hours) and subsequently treated with an anti–IFN-β antibody and rechallenged with LPS. Antibody treatment reduced STAT1 phosphorylation and iNOS protein levels (Figure 4F), which showed that IFN-β neutralization reverts the M1 proinflammatory phenotype of *P21*⁻/⁻ macrophages to a tolerant state, even when antibody is delivered after LPS tolerization. The data suggest that elevated IFN-β is a determining factor in compromising the hyporesponsiveness of *P21*⁻/⁻ macrophages, and acts at all stages of the tolerization process.

IFN-β drives M1 features after LPS tolerance of macrophages (12), while in another system it appeared to reduce TNF-α production (60). To test directly whether IFN-β affects macrophage

reprogramming, we treated WT macrophages with IFN-β during the LPS tolerization period. Treatment was initiated 4 hours after adding LPS and lasted 16 hours, after which cell cultures were washed and rechallenged with LPS. IFN-β had a notable effect on M1 to M2 polarization, as it significantly increased M1 factors such as iNOS and CXCL11 (Figure 4G) while downregulating expression of major M2 components such as CCL17 and CCL22 (Figure 4G). IFN-β treatment had no effect on arginase I or TNF-α expression after secondary LPS activation. Thus, increased IFN-β production impairs M1 to M2 macrophage reprogramming after LPS tolerization and rechallenge, which favors an M1 macrophage phenotype and disrupts essential aspects of M2 transition and tolerization in *P21*⁻/⁻ macrophages.

We tested whether skewing *P21⁻/⁻* macrophages towards an M1 phenotype using IFN-β has a functional effect on disrupting their hyporesponsiveness and tolerization. *P21⁻/⁻* mice, which fail to develop tolerance after 2 consecutive LPS challenges (see Figure 1A), were treated with anti-IFNAR antibody 2 hours before secondary LPS delivery. In accordance with our findings that IFN-β neutralization promotes in vitro tolerization of *P21⁻/⁻* macrophages, in vivo anti-IFNAR treatment induced tolerance and significantly improved *P21⁻/⁻* mouse survival after dual LPS injection (Figure 4H). The data show that the inability of *P21⁻/⁻* macrophages to achieve a hyporesponsive state is associated with their elevated IFN-β production.

p21 attenuates IFN-β expression by regulating the balance of p50-p50 and p65-p50 NF-κB. To understand how lack of p21 mediates increased IFN-β production after repeated LPS stimulation in macrophages, we examined pathways that regulate this cytokine. IFN-β expression can be activated in a MyD88-independent or -dependent manner, through IRF3 or NF-κB, respectively (36). Analysis of the MyD88-independent pathway showed no detectable change in IRF3 phosphorylation in LPS-activated or in LPS-tolerized/LPS-restimulated WT or *P21⁻/⁻* macrophages (Supplemental Figure 9A), which suggests that lack of p21 does not affect this pathway. Analysis of downstream activation indicators of the MyD88-dependent pathway such as ERK and JNK phosphorylation showed no differences after primary and secondary LPS challenge in WT and *P21⁻/⁻* cells (Supplemental Figure 9A). As IRAK-M negatively regulates the TLR4 pathway implicated in LPS tolerance (27), we examined whether p21 deficiency affects this regulator, and found no differences in IRAK-M expression after LPS tolerization and rechallenge (Supplemental Figure 9B).

In agreement with our previous data showing that p21 deficiency increases NF-κB activity after primary LPS treatment (46), we found increased IκBα degradation in *P21⁻/⁻* compared to WT macrophages after primary activation (Supplemental Figure 9A). However, IκBα levels were similar in WT and *P21⁻/⁻* macrophages after LPS rechallenge, which indicates that lack of p21 does not affect NF-κB activation in LPS-tolerized macrophages.

Following LPS tolerization, p50-p50 homodimers repress NF-κB target gene transcription (30). We hypothesized that p21 loss would affect the balance of p65-p50 and p50-p50 NF-κB complexes in favor of p65-p50, thus disrupting macrophage polarization and tolerance. We tested this in supershift analysis using a [³²P]-labeled consensus NF-κB sequence probe and antibodies specific for p65 and p50 NF-κB subunits. We examined NF-κB activation and the composition of NF-κB dimers at different time points after primary LPS activation (15 and 30 minutes and 1, 2, and 4 hours). As early as 15 minutes after primary LPS activation, NF-κB activation was much higher in *P21⁻/⁻* macrophages compared to WT cells (Figure 5A; compare lanes 2 and 5), in accordance with previous findings (46). Anti-p50 antibody supershifted the entire complex (Figure 5A, lanes 3 and 6), consistent with the fact that TLR signaling activates mostly p65-p50 and p50-p50 NF-κB (61). By contrast, anti-p65 antibody supershifted only the p65-p50 portion of the DNA-protein complex, while the p50-p50 portion was unaffected; this permitted quantification of the relative presence of p65-p50 versus p50-p50 complexes (Figure 5A; lanes 4 and 7). The pattern of NF-κB subunit composition was similar in WT and

P21⁻/⁻ LPS-activated macrophages, although at 1 hour after stimulation, the lack of p21 led to a lower proportion of p50-p50 and higher proportion of p65-p50, which reflected greater activation potential (Figure 5A). Thus, during primary LPS activation, lack of p21 increased overall NF-κB activity, as previously demonstrated (46), but also had a previously unknown effect in potentiating p65-p50 predominance over the inhibitory p50-p50 NF-κB.

We performed similar experiments to determine whether lack of p21 influenced the NF-κB activity and its subunit composition at different times after secondary LPS stimulation of tolerized macrophages. In contrast to the data obtained after primary LPS activation, NF-κB activation was similar in WT and *P21⁻/⁻* LPS-tolerized macrophages at all times after secondary stimulation; the results at 15 minutes after LPS rechallenge are shown in Figure 5B (compare lanes 2 and 5). The relative presence of p65-p50 versus p50-p50 complexes was estimated by supershift analysis after secondary LPS treatment in WT and *P21⁻/⁻* macrophages (Figure 5B; lanes 4 and 7). For WT macrophages, a predominance of p50-p50 inhibitory homodimers over p65-p50 complexes was observed at all time points (Figure 5B), which corroborated the compromised inflammatory status of tolerized macrophages. In the case of *P21⁻/⁻* macrophages, the profile of NF-κB complex composition differed, with higher levels of p65-p50 than p50-p50 complexes at 15 minutes after secondary stimulation (Figure 5B). At later times, however, the relative proportion of these complexes reverted to that of WT macrophages (Figure 5B). These findings suggest that the inability of *P21⁻/⁻* macrophages to achieve an M2 phenotype after secondary LPS stimulation is linked to altered balance of NF-κB complexes in these cells.

In previous experiments (Figure 4), we showed that IFN-β levels were essential for the augmented response of *P21⁻/⁻* macrophages after LPS tolerization and rechallenge. To determine how NF-κB composition affects *Ifnb* gene expression, we used the NF-κB element from the *Ifnb* promoter (62), which differs from the consensus NF-κB sequence, and estimated the effect of NF-κB activation on IFN-β regulation.

Analysis of our data using an IFN-β–specific NF-κB probe showed a striking difference in the composition of p65-p50 and p50-p50 complexes in *P21⁻/⁻* compared to WT macrophages after secondary LPS stimulation. At 30 minutes after stimulation we observed the most evident difference, with a clear shift in p50-p50 prevalence in WT macrophages to p65-p50 predominance in *P21⁻/⁻* cells (Figure 5C, compare lanes 4 and 7). In *P21⁻/⁻* macrophages, p65-p50 heterodimers were present at much higher proportion at 15 minutes and predominated for at least 1 hour after secondary LPS treatment (Figure 5C), compared to WT rechallenged macrophages. Apart from these differences in NF-κB complex composition, the overall NF-κB activation was similar for WT and *P21⁻/⁻* macrophages at all time points after rechallenge; the results at 30 minutes after LPS rechallenge are shown (Figure 5C; lanes 2 and 5). The NF-κB subunit-binding pattern was much more affected by the lack of p21 for the *Ifnb* promoter–specific DNA than for the consensus sequence probe (Figure 5, B and C). This might be due to the different binding affinities of p65-p50 and p50-p50 NF-κB for the 2 NF-κB–binding sequences (63).

Overall, our results show that lack of p21 affects the degree of NF-κB activation in macrophages after primary, but not follow-
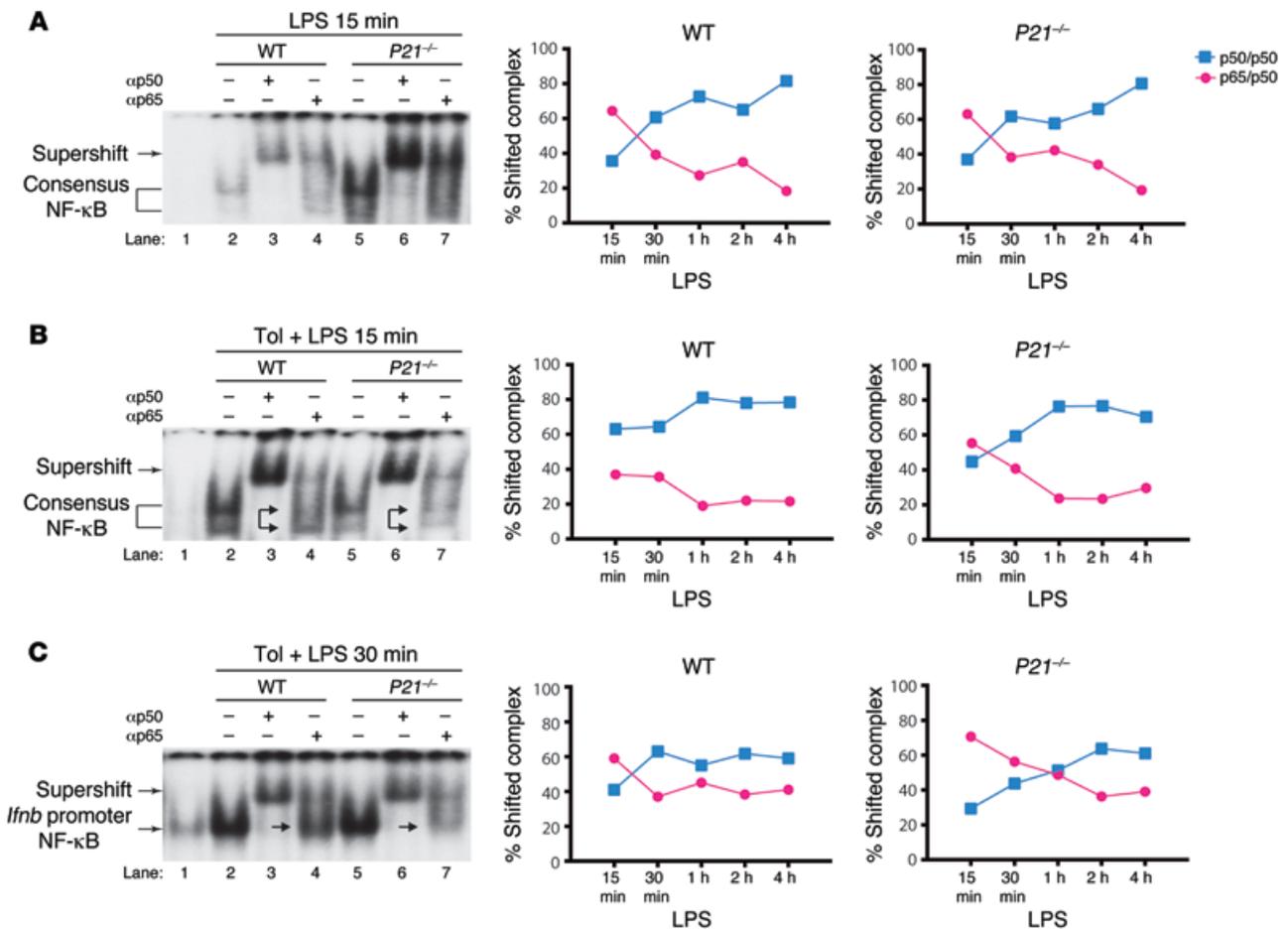
Figure 5. p21 modulates the balance between p65-p50 and p50-p50 NF-κB dimers in LPS-tolerized macrophages. WT and *P21⁻/⁻* resting or tolerized (20 hours) peritoneal macrophages were stimulated with LPS (4 hours). NF-κB complexes that bound the consensus or the *Ifnb* promoter sequence were analyzed by EMSA. Anti–p50 and –p65 NF-κB antibodies were used for supershift analysis. Supershift intensity was assessed by densitometry and plotted as the percentage of supershifted complex at indicated times after LPS stimulation. (**A**) Left, Increased NF-κB binding to the consensus sequence in *P21⁻/⁻* (lane 5) compared with WT (lane 2) LPS-activated macrophages (shown at 15 minutes). Right, Relative NF-κB complex composition at different times after LPS activation. (**B**) Left, Similar NF-κB binding to the consensus sequence in WT (lane 2) and *P21⁻/⁻* (lane 5) LPS-tolerized macrophages (shown at 15 minutes) and reduced p50-p50 DNA binding in *P21⁻/⁻* macrophages as indicated by arrows (compare lanes 4 and 7). Right, Delayed switch to p50-p50 NF-κB complex composition in *P21⁻/⁻* LPS-tolerized macrophages. (**C**) Left, Similar NF-κB binding to the *Ifnb* promoter sequence in WT (lane 2) and *P21⁻/⁻* (lane 5) macrophages after LPS restimulation (shown at 30 minutes) and reduced p50-p50 DNA binding in *P21⁻/⁻* macrophages (compare lanes 4 and 7; arrow). Right, Delayed switch to p50-p50 NF-κB complexes bound to the *Ifnb* promoter sequence in *P21⁻/⁻* LPS-tolerized macrophages. In all gels, the first lane is nuclear extract of untreated macrophages (negative control). Representative results of 2 independent experiments are shown.

ing secondary LPS treatment. Instead, lack of p21 after restimulation disrupts the accumulation of p50-p50 homodimers that limit proinflammatory responses and IFN-β expression. p21 therefore promotes M1 to M2 macrophage reprogramming through a mechanism that incites p50-p50 NF-κB prevalence and limits IFN-β production.

Loss of p21 decreases DNA-binding affinity of inhibitory p50-p50 NF-κB homodimers. Our data show that p21 deficiency impairs the accumulation of inhibitory p50-p50 homodimers at NF-κB binding sites and leads to predominance of activating p65-p50 NF-κB. We therefore asked how p21 regulates the balance between p65-p50 and p50-p50 NF-κB dimers in tolerized macrophages. The BCL3 protein mediates LPS tolerance by stabilizing the DNA-bound p50-p50 complex and protecting it from ubiquitination and degradation (64). Although p50-p50 binds with the same affinity to DNA, its subsequent ubiquitina-

tion and degradation is enhanced in the absence of BCL3, which leads to p65-p50 dimer prevalence and compromised LPS tolerance. As *P21⁻/⁻* macrophages also showed reduced p50-p50 DNA binding, we evaluated whether these events are associated with enhanced p50 ubiquitination.

In accordance with its role in DNA-bound p50-p50 stabilization, we detected BCL3 only in nuclear extracts; however, both mRNA and protein levels of BCL3 and p105 (the p50 precursor) were similar in *P21⁻/⁻* and WT LPS-rechalleged macrophages (Figure 6, A and B). We next examined whether p21 deficiency affects p50 ubiquitination. Surprisingly, we found a large reduction in p50 ubiquitination in *P21⁻/⁻* compared to WT macrophages at 30 minutes and 1 hour after LPS rechallenge (Figure 6C). These data demonstrate that decreased DNA-bound p50-p50 in *P21⁻/⁻* macrophages was not caused by increased ubiquitination and degradation, dismissing a possible association of p21 with the
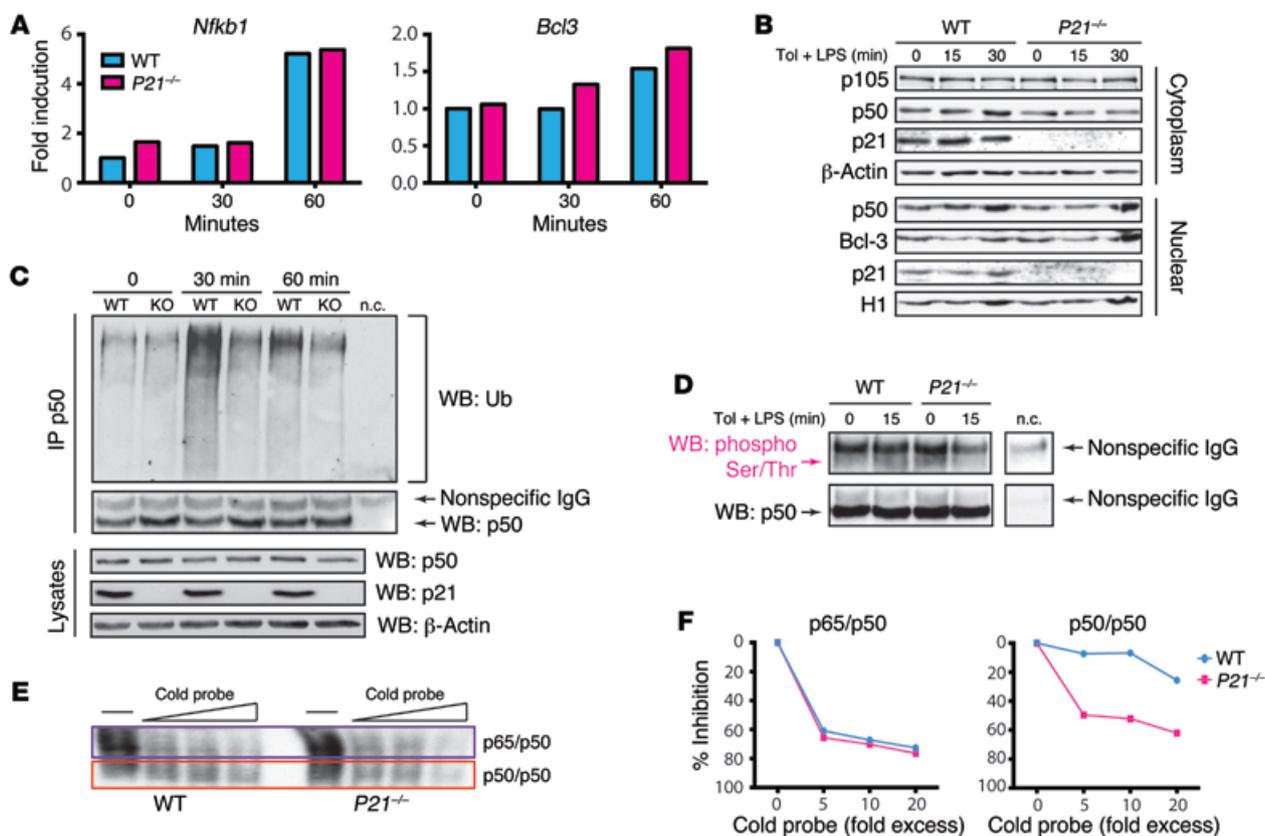
Figure 6. p21 regulates p50-p50 NF-κB DNA binding. (**A**) RT-PCR analysis showing similar *Nfkb1* (encoding p105) and *Bcl3* gene expression in WT and *P21−/−* LPS-tolerized/restimulated peritoneal macrophages. Results were normalized to β-actin and show fold induction over unstimulated WT cells. Data are representative of 3 independent experiments. (**B**) Immunoblot showing similar p50 protein levels in the cytoplasmic and nuclear fractions of WT and *P21−/−* LPS-tolerized/restimulated peritoneal macrophages. β-Actin and histone H1 were used as loading controls for the cytoplasmic and nuclear fractions, respectively. (**C**) Reduced ubiquitination of p50 in *P21−/−* LPS-tolerized/restimulated peritoneal macrophages. Equal amounts of protein were immuno-precipitated with antibody against p50 and immunoblotted with antibody against ubiquitin. n.c., negative control; IP performed in the absence of cell extracts. (**D**) Reduced p50 phosphorylation in *P21−/−* LPS-tolerized/restimulated peritoneal macrophages. Equal amounts of protein were immunoprecipi-tated with antibody against p50 and immunoblotted with antibody against phospho-serine/threonine. (**E**) p21 increases p50 homodimer binding to DNA by increasing its affinity. Tolerized (20 hours) WT and *P21−/−* peritoneal macrophages were stimulated with LPS (15 minutes). Anti–p50 NF-κB antibody was used for supershift assays with increasing amounts of unlabeled oligonucleotide (cold probe), and NF-κB complexes binding the *Ifnb* promoter sequence were analyzed by EMSA. (**F**) p50-p50 and p65-p50 DNA binding was measured by densitometry of autoradiogram in **E**. Shown are representative gels of at least 2 experiments performed.

BCL3-dependent pathway. The decreased ubiquitination in *P21−/−* macrophages correlated with lower proportions of DNA-bound p50-p50 at these times (Figure 5C).

As DNA binding precedes p50 ubiquitination (64), we considered that p21 deficiency could decrease p50-p50:DNA binding affinity, resulting in reduced p50 ubiquitination. Efficient DNA binding of p50-p50, but not of p65-p50, depends on p50 phosphorylation (65). Indeed, p50 phosphorylation was reduced in *P21−/−* macrophages at 15 minutes after LPS rechallenge (Figure 6D), suggesting that lack of p21 decreases p50-p50 DNA-binding affinity.

To obtain direct evidence for p21-dependent regulation of p50-p50 DNA-binding affinity after LPS rechallenge, we used EMSA supershift assays to analyze p65-p50 and p50-p50 DNA-binding affinities for the NF-κB element of the *Ifnb* promoter (Figure 6E). Intriguingly, we found that p21 deficiency acutely reduced the DNA-binding affinity of p50-p50 homodimers without affecting p65-p50 affinity (Figure 6F). p21 thus promotes p50-p50 NF-κB inhibitory activity during LPS tolerance by increasing its

p50 DNA-binding affinity. These findings describe an alternative route by which p50-p50 could affect tolerance induction.

Regulation of IFN-β by p21 in human monocyte hyporesponsiveness and in sepsis. To evaluate the relevance of our findings in human inflammatory responses, we sought to determine the role of p21 in the hyporesponsive status of monocytes from 7 patients suffering sepsis secondary to urinary tract infection. Patient monocytes are immunosuppressed, and do not upregulate proinflammatory cytokines when challenged with LPS ex vivo (21, 66), a state that resembles LPS tolerance. Compared to healthy cells, monocytes from sepsis patients (Supplemental Table 1) expressed significantly higher p21 levels (Figure 7A). This suggests that high p21 expression could control human monocyte hyporesponsiveness in sepsis and associate with low IFN-β levels. In fact, monocytes from sepsis patients showed an overall low IFN-β expression that correlated negatively to p21 expression in a statistically significant manner (Pearson correlation analysis). Thus, patients that upregulated p21 had low IFN-β levels (Figure 7A). This hypore-
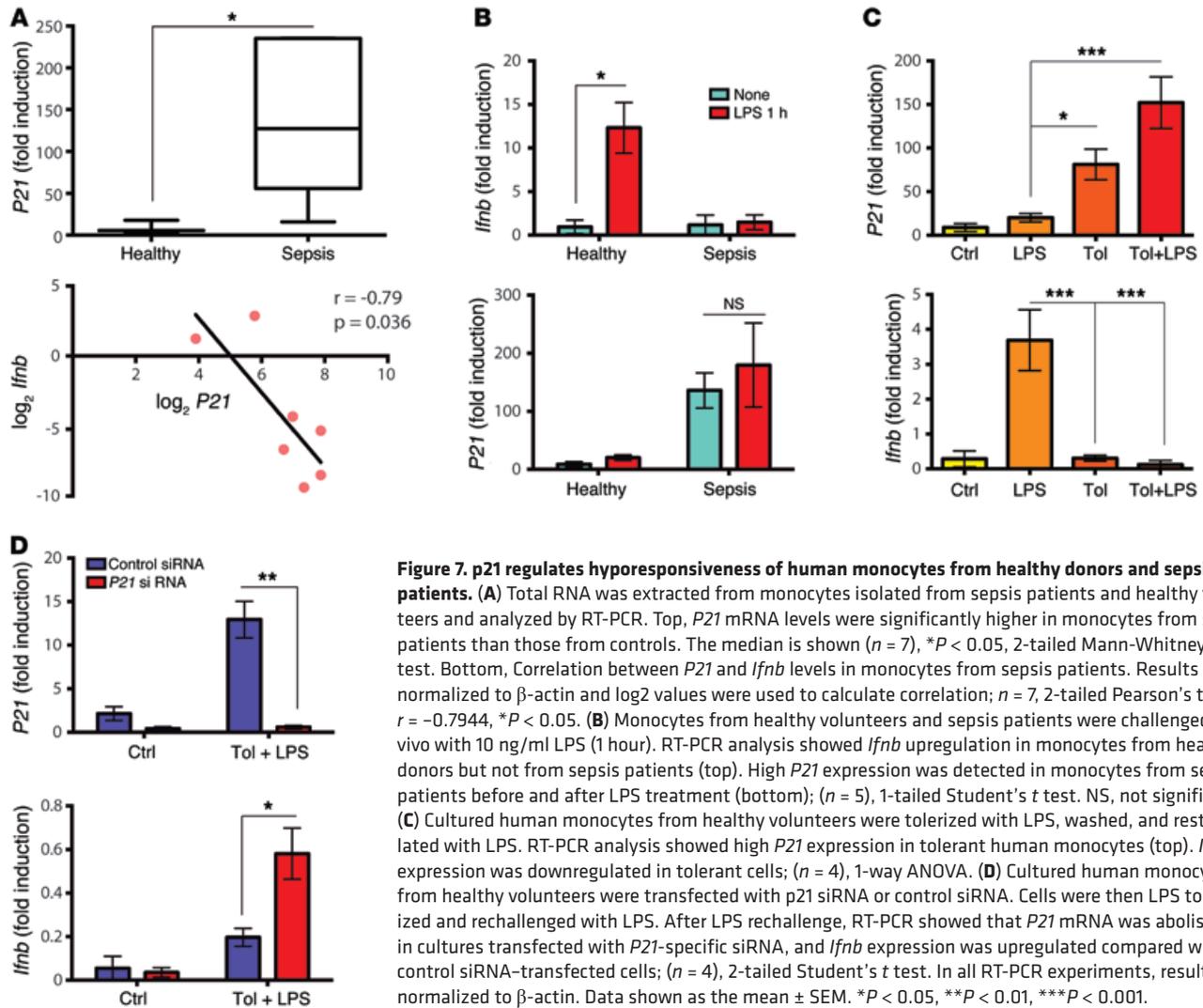
Figure 7. p21 regulates hyporesponsiveness of human monocytes from healthy donors and sepsis patients. (A) Total RNA was extracted from monocytes isolated from sepsis patients and healthy volunteers and analyzed by RT-PCR. Top, *P21* mRNA levels were significantly higher in monocytes from sepsis patients than those from controls. The median is shown (*n* = 7), *P < 0.05, 2-tailed Mann-Whitney *U* test. Bottom, Correlation between *P21* and *Ifnb* levels in monocytes from sepsis patients. Results were normalized to β-actin and log2 values were used to calculate correlation; *n* = 7, 2-tailed Pearson's test *r* = −0.7944, *P < 0.05. **(B)** Monocytes from healthy volunteers and sepsis patients were challenged ex vivo with 10 ng/ml LPS (1 hour). RT-PCR analysis showed *Ifnb* upregulation in monocytes from healthy donors but not from sepsis patients (top). High *P21* expression was detected in monocytes from sepsis patients before and after LPS treatment (bottom); (*n* = 5), 1-tailed Student's *t* test. NS, not significant. **(C)** Cultured human monocytes from healthy volunteers were tolerized with LPS, washed, and restimulated with LPS. RT-PCR analysis showed high *P21* expression in tolerant human monocytes (top). *Ifnb* expression was downregulated in tolerant cells; (*n* = 4), 1-way ANOVA. **(D)** Cultured human monocytes from healthy volunteers were transfected with p21 siRNA or control siRNA. Cells were then LPS tolerized and rechallenged with LPS. After LPS rechallenge, RT-PCR showed that *P21* mRNA was abolished in cultures transfected with *P21*-specific siRNA, and *Ifnb* expression was upregulated compared with control siRNA–transfected cells; (*n* = 4), 2-tailed Student's *t* test. In all RT-PCR experiments, results were normalized to β-actin. Data shown as the mean ± SEM. *P < 0.05, **P < 0.01, ***P < 0.001.

sponsivness of monocytes from sepsis patients was corroborated by significantly impaired TNF-α upregulation in response to LPS in vitro challenge, compared to control cells (Supplemental Figure 10). In addition, LPS stimulation induced high IFN-β expression in monocytes from healthy donors but not from sepsis patients (Figure 7B). p21 levels were high in sepsis monocytes, and LPS treatment did not further increase p21 expression (Figure 7B), which suggests that already high p21 levels were sufficient to maintain their unresponsiveness. It therefore appears that the tolerant phenotype of monocytes in sepsis is linked to high p21 levels, which account for the IFN-β reduction.

In line with the results showing that the hyporesponsivess of monocytes from sepsis patients was associated with high p21 levels, human monocytes from healthy donors showed a notable increase in p21 expression after LPS tolerization or tolerization and rechallenge (Figure 7C). In addition, IFN-β was considerably downregulated after LPS tolerization and rechallenge compared to its high induction after primary LPS activation (Figure 7C). Monocyte hyporesponsiveness after LPS tolerization was also confirmed by TNF-α downregulation and CCL2 upregulation in LPS-tolerized cells (Supplemental Figure 11A). These experiments suggest that p21 is a critical factor in regulating monocyte hypo-

responsiveness and IFN-β expression. LPS tolerization of human monocytes has been associated with their polarization from an M1- to an M2-tolerant state (12); our data therefore indicate that p21 is a regulator of this reprogramming.

To directly show that p21 potentiates the hyporesponsive phenotype of human monocytes, we performed p21 siRNA silencing experiments in monocytes and studied their response to LPS after tolerization. RT-PCR confirmed that *P21* mRNA was abolished in p21 siRNA–transfected LPS-tolerized monocytes (Figure 7D). These monocytes showed a significant increase in *Ifnb* expression compared with controls (Figure 7D), indicating that p21 downregulation allows IFN-β upregulation and halts monocyte hyporesponsiveness. Impaired hyporesponsiveness in *P21*-knocked-down monocytes was further confirmed by increased TNF-α production and decreased antiinflammatory cytokine IL-10 (Supplemental Figure 11B). These data identify p21 as a major player in promoting LPS tolerance in human monocytes by limiting IFN-β expression and their overall inflammatory status.

Since LPS-tolerant monocytes are considered analogous to hyporesponsive sepsis monocytes (22), our results suggest that p21 has a role in establishing immunosuppression in sepsis patient monocytes.

Discussion

Due to their plasticity, macrophages can polarize from an M1 to an M2 phenotype (3, 6, 9) or reprogram from an inflammatory to a hyporesponsive state (19), while maintaining alternative function (13). Immunosuppressed monocytes and macrophages are linked to pathologies such as sepsis, acute coronary syndrome, and cystic fibrosis (18, 67, 68). During sepsis, monocytes undergo an intense proinflammatory response that leads to hyporesponsiveness. Of interest, patient death is associated mainly with the immunosuppressed phase rather than the inflammatory stage, which is similar to LPS-induced septic shock in mice. Previous studies from our group and others showed that, independently of its cell cycle inhibitory role, p21 inhibits LPS-induced proinflammatory macrophage activation and septic shock development (46, 47), although compared to WT, $P21^{-/-}$ unstimulated thioglycollate-elicited macrophages showed a reduced predisposition to inflammation (69). Here we explored whether p21 could affect sepsis by controlling inflammatory macrophage reprogramming to a hyporesponsive phenotype. Since this hyporesponsive state resembles macrophage immunosuppression after LPS tolerization (12), we studied the role of p21 in hyporesponsiveness induction. LPS tolerance results in reprogramming of inflammatory M1 to M2-like macrophages after LPS rechallenge (12, 13). Lack of p21 disrupted LPS macrophage tolerization both in vitro and in vivo and attenuated M1 macrophage reprogramming to M2 hyporesponsiveness. Analysis of this p21 effect led to 3 central conclusions. First, p21 promotes macrophage reprogramming to a hyporesponsive state by downregulating IFN-β. Second, p21 emerges as a regulator of the p65-p50 and p50-p50 NF-κB balance by regulating p50-p50:DNA binding affinity, and downregulates IFN-β expression. Finally, p21 also monitors human monocyte responses, as p21 silencing in these cells augmented IFN-β production and restricted LPS tolerization. These results support a system in which p21 upregulation and IFN-β downmodulation could contribute to induction of hyporesponsiveness in monocytes from sepsis patients.

$P21^{-/-}$ mice do not develop tolerance after LPS priming; after a secondary LPS challenge, they produce larger amounts of TNF-α and IFN-β compared to WT mice, and die. Peritoneal M1 macrophages (49–51) showed greater activation in the absence of p21, suggesting that compromised tolerance could result from failed M1 to M2 polarization. In fact, M1 to M2 macrophage reprogramming is considered essential for in vivo LPS tolerance (12, 13). Reprogrammed M2 cells are nonetheless distinct from the conventional IL-4–dependent, alternatively activated M2 macrophages, which are not implicated in LPS tolerance (70).

M1 to M2 macrophage reprogramming by in vitro LPS tolerization was previously described by Porta et al. (12). After LPS tolerization and rechallenge, $P21^{-/-}$ macrophages produced higher levels of M1-associated cytokines TNF-α and IL-1β than WT cells. Although TNF-α levels were clearly reduced after tolerization in both WT and $P21^{-/-}$ macrophages, IFN-β remained high after tolerization and prior to rechallenge only in $P21^{-/-}$ macrophages. These persisting IFN-β levels, even in the absence of LPS stimulus, suggested that the effect of p21 on IFN-β expression is relevant for tolerance induction. Concurring with this, IFN-β was proposed to attenuate LPS tolerization, since it was expressed highly in $P50^{-/-}$ macrophages that fail to develop LPS tolerance (12).

$P21^{-/-}$ macrophages produce high IFN-β levels after LPS tolerization and do not undergo M1 to M2 polarization. However, neutralization of IFN-β function during the LPS tolerization period allowed $P21^{-/-}$ macrophages to reach a hyporesponsive state after LPS rechallenge by limiting M1 activation and promoting expression of M2 markers. Even when IFN-β activity was neutralized only throughout the LPS rechallenge, $P21^{-/-}$ macrophage responses such as STAT1 phosphorylation and iNOS induction were reduced. Increased IFN-β production by $P21^{-/-}$ macrophages appear to play a unique role in disrupting their polarization to an M2-like hyporesponsive state, since TNF-α neutralization reduced iNOS induction only moderately and had no effect on M2-associated molecules. IFN-β treatment of WT macrophage cultures during tolerization interrupted their M1 to M2 reprogramming, as macrophages adopted a more pronounced M1 phenotype and reduced M2 characteristics. The role of IFN-β in impairing $P21^{-/-}$ macrophage tolerization was further validated in an in vivo LPS tolerance setting, in which neutralization of the IFN-β receptor prior to LPS rechallenge significantly improved survival of $P21^{-/-}$ mice. Together, these data indicate that p21 promotes M1 to M2 macrophage reprogramming by downmodulating IFN-β production.

Mechanisms that drive unresponsiveness of macrophages in mice and of monocytes in humans differ, and several molecules reported as mediators of LPS tolerance in mice (such as SHIP, SOCS1, and A20) (28, 71) are not relevant in humans (72, 73). Moreover, systemic genomic analysis in human and mouse inflammatory diseases, including endotoxemia, showed very low gene correlation between humans and mouse models (74). It was therefore essential to show that p21 expression drives M2 hyporesponsiveness in human monocytes. After LPS tolerization and rechallenge, human monocytes showed heightened p21 levels, which lowered IFN-β expression. This p21 function was validated directly, since $P21$ knockdown reversed the hyporesponsive phenotype of LPS-tolerized human monocytes, which had high IFN-β levels. In line with the analogous state between LPS tolerance and monocyte hyporesponsiveness in sepsis (19), p21 was strongly upregulated in refractory patient–derived monocytes, while IFN-β was downmodulated. Statistical analysis indicated a significant negative correlation between p21 and IFN-β levels. These data suggest that p21 is a key factor in driving macrophage hyporesponsiveness in human disease by reducing IFN-β levels.

Although the IFN-β requirement has been clearly established in viral infection, its role in bacterial infection remains undefined (75). In addition to its proinflammatory effect, an immunosuppressive role has also been attributed to IFN-β (76), and these complex effects have been pointed out for inflammation and septic shock (53).

Septic shock induction in mice requires IFN-β, as shown by studies with IFN-β and IFN-β receptor (IFNAR) knockout mice (77, 78) and other mouse models that regulate IFN-β expression (79, 80). It was therefore proposed that IFN-β targeting in human sepsis might have a therapeutic benefit (80). In contrast to its proinflammatory role, IFN-β might trigger monocyte immunosuppression in endotoxin tolerance (34), and its delivery severely reduced septic shock development in mice (76). Due to these contrasting effects, limiting IFN-β signaling for therapeutic purposes entails conceptual difficulties. Our results showing that p21-dependent

IFN-β downmodulation drives monocyte hyporesponsiveness discourage IFN-β reduction–based treatment in sepsis, as it could further deteriorate responses to secondary infections.

p21 negatively regulates the NF-κB activation pathway after primary LPS activation (46). Nevertheless, p21 had no effect on this activation in LPS tolerance, and $P21^{-/-}$ and WT macrophages showed similar NF-κB activation after rechallenge. Through our data, however, we identified a previously unrecognized role for p21 in regulating the balance between p65-p50 and p50-p50 dimers.

Accumulation of NF-κB p50-p50 was proposed to drive macrophage immunosuppression (30) and $P50^{-/-}$ murine macrophages failed to develop LPS tolerance (26, 81). LPS tolerance, which induces M1 to M2 macrophage reprogramming, is driven by the increase in inhibitory p50-p50 over p65-p50 NF-κB dimers (12). In our system, lack of p21 impaired the reprogramming of M1 to immunosuppressed M2 macrophages by sustaining low p50-p50 levels and predominant p65-p50 complexes. After secondary LPS restimulation, $P21^{-/-}$ macrophages showed a notable alteration in the pattern of p65-p50 versus p50-p50 products bound to the NF-κB consensus sequence, with a reduction in p50-p50 DNA-bound complexes. This accounted for the increased production of consensus sequence–dependent products such as TNF-α. We further showed that after primary LPS stimulation, in which p21 regulates overall NF-κB activation, p21 also regulates the p65-p50 and p50-p50 balance later in activation. p21 thus has a dual role in NF-κB regulation; first, it suppresses the NF-κB activation pathway after LPS stimulation and second, it blunts NF-κB activity by promoting inhibitory p50-p50 complexes, tolerance, and M2 macrophage polarization.

To understand how p21 deficiency drives IFN-β, we examined the relative binding of p65-p50 versus p50-p50 NF-κB to a promoter sequence of *Ifnb* that holds specific differences from the NF-κB consensus sequence (62). We detected increased p65-p50 bound to the IFN-β promoter in $P21^{-/-}$ as compared to WT rechallenged macrophages, while p50-p50 binding was proportionally decreased. This result justified the increase in IFN-β by rechallenged $P21^{-/-}$ macrophages and confirmed the role of p21 in modulating IFN-β production. In the absence of p21, the *Ifnb* promoter sequence showed higher p65-p50 and lower p50-p50 binding compared to the NF-κB consensus sequence, which could be explained by the higher affinity of p65-p50 for the *Ifnb* promoter than for the consensus sequence; the opposite occurs for p50-p50 binding ability (63). Our data indicate that p21 deficiency shifts the p65-p50 and p50-p50 balance toward active p65-p50 NF-κB complexes, which affects the expression of IFN-β among other molecules.

Previous studies indicated that p65-p50 overexpression might drive p50-p50 accumulation during LPS tolerance (30). Interaction of BCL3 with p50-p50 is a major pathway that enhances the inhibitory effect of p50/p50 on NF-κB, as it stabilizes binding of the homodimer (64, 82, 83). In BCL3-deficient macrophages, p50-p50 ubiquitination is enhanced, and results in p50-p50 degradation and deficient LPS tolerance (64). Instead, we show decreased p50-p50 ubiquitination in p21-deficient macrophages, and thus rule out similarities with the $Bcl3^{-/-}$ system. We demonstrated that in $P21^{-/-}$ macrophages, p50-p50:DNA binding affinity is impaired, which leads to reduced binding of p50-p50 but not

of p65-p50. This finding explains the prevalence of DNA-bound p65-p50 over p50-50 in $P21^{-/-}$ macrophages after secondary LPS stimulation. The reduced p50-p50 binding affinity can be associated with p50 phosphorylation, a posttranslational modification associated with p50-p50 DNA-binding capacity (65). p21 can thus be envisaged as a modulator of macrophage regulatory upstream events that control posttranslational modifications of p50 and control its binding affinity to NF-κB DNA-binding sites.

We show here that $P21^{-/-}$ macrophages fail to polarize from an M1 to an M2 state after LPS rechallenge. A role was reported for p21 in atherosclerosis, as this disease is reduced in $ApoE^{-/-}P21^{-/-}$ mice; the authors elegantly showed that increased apoptosis of $P21^{-/-}$ macrophages in lesions characterized this model (69). Nevertheless, a role for p21 in M1 macrophage polarization to M2 status was not shown for this model. As endotoxin tolerance and atherosclerosis are entirely different inflammation models, p21 may have distinct effects in each case.

Our data show that p21 deficiency disrupts M1 to M2 polarization. It could then be hypothesized that the reduced disease in $ApoE^{-/-}P21^{-/-}$ mice is related to the M2 cell impairment, given the possible proatherosclerotic potential of M2 macrophages (84); this would challenge the classical inflammation-resolving role of M2 macrophages (85, 86). Given the complexity of atherosclerosis development, further research is needed to assign a role for p21 in M1 to M2 reprogramming in atherosclerosis.

We show that p21 modulates the equilibrium between p50-p50 and p65-p50 NF-κB by promoting inhibitory p50-p50 binding to DNA. These data reveal a role for p21 in fine-tuning the balance of NF-κB products and in promoting macrophage hyporesponsiveness, distinct from its previously known role as a suppressor of the NF-κB activation pathway after macrophage stimulation. p21 is thus a major factor in potentiating p50-driven control of inflammation and a key molecule in regulating macrophage transition from a proinflammatory to a hyporesponsive state. Since regulation of this transition could be of therapeutic value for sepsis treatment, understanding the role of p21 could assist in defining molecular aspects of monocyte reprogramming and in discovering new targets for sepsis treatment.

Methods

Animals. Mice were maintained in the barrier zone of our animal facility. Six- to eight-week-old female $P21^{-/-}$ and control mice were used for all experiments. C57BL/6 mice were from Harlan Interfauna Ibérica; $P21^{-/-}$ mice were previously described (46).

Induction of LPS tolerance in vivo. Mice were injected i.p. with 30 μg LPS (from *E. coli* 0127:B8), followed 16 hours later by an i.v. injection of 150 μg LPS. Survival was monitored for 72 hours. To obtain serum, at 2 hours after LPS rechallenge, peritoneal exudates were harvested and blood collected by cardiac puncture. For the IFNAR-blocking experiments, $P21^{-/-}$ mice (*n* = 9/group) were injected i.p. with 300 μg IFNAR1 monoclonal antibody (MAR1-5A3, BioXCell) or a control IgG antibody (MOPC-21; BioXCell/fg345) 2 hours before LPS rechallenge.

Serological analysis. We tested mouse blood serum and cell-free culture supernatants by ELISA for TNF-α (PeproTech), IFN-β (PBL Assay Science), and CCL17 (R&D Systems) levels. Cytokine levels in culture supernatants of the human samples were determined using the cytometric bead array (CBA) Flex Set (BD Biosciences) following the

manufacturer's protocol. Data were collected and analyzed using a BD FACSCalibur flow cytometer (BD Biosciences).

Intracellular cytokine staining. For intracellular cytokine detection, mice were injected i.v. with brefeldin A (500 μl 1× brefeldin A in PBS; BioLegend) 30 minutes after LPS rechallenge. After 3 hours, splenocytes and peritoneal exudate were harvested and stained with a Violet LIVE/DEAD Stain Kit (Invitrogen) to exclude dead cells. After surface marker staining with anti–CD11b-PE-Cy7 (M1/70; BioLegend), –F4/80-APC (BM8; eBioscience), –CD4-PeCy7 (GK 1.5; BioLegend) and –CD8-PerCP (53-6.7; BioLegend), cells were washed with PBS, fixed, and permeabilized with a Cytofix/Cytoperm kit (BD Biosciences) and blocked with 1 μl Fc receptor–blocking antibody (082732121; Beckman Coulter; 15 minutes, 4°C). Cells were stained intracellularly with anti–TNF-α-PE (MP6-XT22; 1/100; eBioscience) and –IFN-γ-APC (XMG1.2; 1/100; eBioscience) and analyzed on a Gallios cytometer (Beckman Coulter).

Culture and treatment of mouse peritoneal macrophages. Peritoneal exudate cells (PECs) were harvested from mice 4 days after i.p. administration of 1 ml 3% thioglycollate medium (Difco). PECs were cultured (2 hours) in RPMI 1640 supplemented with ʟ-glutamine, nonessential amino acids, 1 mM sodium pyruvate, 1 mM HEPES, 2-mercaptoethanol, and penicillin/streptomycin. Nonadherent cells were removed by washing with PBS; adherent macrophages were cultured overnight in complete RPMI 1640 with 10% FBS. To establish tolerance, cells were treated with LPS (100 ng/ml; *E. coli* 0127:B8; Sigma-Aldrich) for 20 hours, washed with PBS, maintained in medium for 2 hours, and then restimulated with LPS (100 ng/ml) for 4 hours (12). Control cells were tolerized with LPS (20 hours), washed, and maintained in medium for 6 hours without LPS rechallenge. To induce LPS activation, cells were incubated in medium for 20 hours, washed, cultured in medium for 2 hours, and stimulated with LPS for 4 hours. Unstimulated cells were maintained in medium throughout the experiment. Depletion assays were performed by incubating cells with rat IgG1 anti–IFN-β antibody (7F-D3; Yamasa Corporation), rat IgG1 anti–TNF-α antibody (XT3.11; BioXCell), or isotype control (CN210020; rat IgG1, Antigenix America) at a concentration of 6.7 μg/ml. WT cells were treated with IFN-β (100 U/ml; PBL Assay Science) initiated 4 hours after adding primary LPS.

Immunoprecipitation. Macrophages were lysed in RIPA buffer (radioimmunoprecipitation assay buffer) supplemented with 1× protease/phosphatase inhibitor cocktail (Roche). Equal amounts of protein were precleared with Protein G Dynabeads (Invitrogen), immunoprecipitated with an anti-p50 antibody (D-17; Santa Cruz Biotechnology), and analyzed by Western blot using anti–phospho (Ser/Thr) PKA substrate antibodies (9621; Cell Signaling Technology).

Ubiquitination assay. To detect p50 ubiquitination we used a previously described protocol (64). Briefly, macrophage cultures were incubated with proteasome inhibitor MG132 (20 μM; 30 minutes, 37°C) before harvest, washed in PBS/10 μM *N*-ethylmaleimide (N-EM), lysed in 1% SDS supplemented with 1× protease/phosphatase inhibitor cocktail by boiling for 5 minutes, and diluted (1/10) in RIPA buffer supplemented with 20 μM N-EM and 1× protease/phosphatase inhibitor cocktail. Equal amounts of protein were precleared with Protein G Dynabeads and immunoprecipitated with an anti-p50 antibody (D-17). After SDS-PAGE, proteins were transferred to a nitrocellulose membrane, autoclaved (40 minutes), and immunoblotted with an anti-Ub antibody (P4D1; Santa Cruz Biotechnology) to detect p50 ubiquitination.

Patients. We included 7 subjects with sepsis secondary to a urinary tract infection (clinical details in Supplemental Table 1) who were admitted to the Department of Internal Medicine Service at La Paz Hospital (Madrid, Spain). The patients met the consensus definition of sepsis (87) and sepsis was confirmed by blood cultures positive for *E. coli*. Peripheral blood was collected within 24 hours of sepsis confirmation. Exclusion criteria included presence of malignancy or chronic inflammatory diseases, treatment with steroids or immunosuppressive drugs during the last month, hepatic failure (serum aspartate aminotransferase and/or alanine aminotransferase > 100 IU/l; prothrombin activity < 60%; total bilirubin < 60 μmol/l), renal insufficiency (plasma creatinine > 200 μmol/l), HIV/AIDS, hepatitis B or C, pregnancy, and age > 80 years. Blood collected from healthy volunteers served as controls.

Isolation and culture of human monocytes. Monocytes were obtained from peripheral blood and purity was tested as described (16). To establish endotoxin tolerance, monocytes were tolerized with 10 ng/ml LPS (16 hours), washed with PBS, and rechallenged with 10 ng/ml LPS for indicated times. Control cells were not tolerized or rechallenged with LPS.

EMSA supershift. EMSA analysis for NF-κB binding to consensus or *Ifnb* promoter sequences is described in Supplemental Materials and Methods. For supershift analysis, 1 μg of antibody against p50 (D-17) or p65 (F-6) NF-κB (Santa Cruz Biotechnology) was added to the reaction mixture at room temperature for 20 minutes before addition of radiolabeled probes. Binding reactions were resolved in a 4% nondenaturing polyacrylamide gel (300 V, 1.5 hours, 4°C) in 0.5× TBE. Gels were then dried and exposed to X-ray film at –80°C. Densitometry was performed using Quantity One 4.6.6 software (Bio-Rad). Alternatively, gels were exposed to a phosphor screen and visualized on a Personal Molecular Imager (Bio-Rad) and similar data were obtained.

Statistics. Statistical significance was determined by unpaired 2-tailed Student's *t* test or by 1-way ANOVA (with Bonferroni correction). Survival curves were generated using the Kaplan-Meier method, and compared using the log-rank test. Correlation analysis was assessed using the Pearson correlation coefficient. All statistical analyses were conducted using Prism 6.0 software (GraphPad). $*P < 0.05$, $**P < 0.01$, $***P < 0.001$.

Study approval. All animal experiments were designed in compliance with European Union directives and guidelines and were approved by the Centro Nacional de Biotecnología (CNB-CSIC) Ethics Committee. All participant patients gave informed consent. The study was performed in accordance with the Helsinki Declaration of 2000 and was approved by the Hospital La Paz Ethics Committee.

Author contributions

Acknowledgments

Address correspondence to: Dimitrios Balomenos, Department of Immunology and Oncology, Centro Nacional de Biotecnología (CNB-CSIC), Darwin 3, Campus de Cantoblanco, 28049 Madrid, Spain. Phone: 34.91.585.5449; E-mail: dbalomenos@cnb.csic.es.

1. Gordon S, Taylor PR. Monocyte and macrophage heterogeneity. *Nat Rev Immunol*. 2005;5(12):953–964.

2. Lawrence T, Natoli G. Transcriptional regulation of macrophage polarization: enabling diversity with identity. *Nat Rev Immunol*. 2011;11(11):750–761.

3. Mosser DM, Edwards JP. Exploring the full spectrum of macrophage activation. *Nat Rev Immunol*. 2008;8(12):958–969.

4. Biswas SK, Mantovani A. Macrophage plasticity and interaction with lymphocyte subsets: cancer as a paradigm. *Nat Immunol*. 2010;11(10):889–896.

5. Gordon S, Martinez FO. Alternative activation of macrophages: mechanism and functions. *Immunity*. 2010;32(5):593–604.

6. Mills C. M1 and M2 macrophages: oracles of health and disease. *Crit Rev Immunol*. 2012;32(06):463–488.

7. Mantovani A, Sica A, Sozzani S, Allavena P, Vecchi A, Locati M. The chemokine system in diverse forms of macrophage activation and polarization. *Trends Immunol*. 2004;25(12):677–686.

8. Edwards JP, Zhang X, Frauwirth KA, Mosser DM. Biochemical and functional characterization of three activated macrophage populations. *J Leukoc Biol*. 2006;80(6):1298–1307.

9. Sica A, Mantovani A. Macrophage plasticity and polarization: in vivo veritas. *J Clin Invest*. 2012;122(3):787–795.

10. Satoh T, et al. Critical role of Trib1 in differentiation of tissue-resident M2-like macrophages. *Nature*. 2013;495(7442):524–528.

11. Mantovani A, Sozzani S, Locati M, Allavena P, Sica A. Macrophage polarization: tumor-associated macrophages as a paradigm for polarized M2 mononuclear phagocytes. *Trends Immunol*. 2002;23(11):549–555.

12. Porta C, et al. Tolerance and M2 (alternative) macrophage polarization are related processes orchestrated by p50 nuclear factor kappaB. *Proc Natl Acad Sci U S A*. 2009;106(35):14978–14983.

13. Pena OM, Pistolic J, Raj D, Fjell CD, Hancock RE. Endotoxin tolerance represents a distinctive state of alternative polarization (M2) in human mononuclear cells. *J Immunol*. 2011;186(12):7243–7254.

14. Foster SL, Hargreaves DC, Medzhitov R. Gene-specific control of inflammation by TLR-induced chromatin modifications. *Nature*. 2007;447(7147):972–978.

15. Piao W, et al. Endotoxin tolerance dysregulates MyD88- and Toll/IL-1R domain-containing adapter inducing IFN-beta-dependent pathways and increases expression of negative regulators of TLR signaling. *J Leukoc Biol*. 2009;86(4):863–875.

16. Cubillos-Zapata C, et al. NFκB2/p100 is a key factor for endotoxin tolerance in human monocytes: a demonstration using primary human monocytes from patients with sepsis. *J Immunol*. 2014;193(8):4195–4202.

17. Cavaillon JM, Adib-Conquy M. Bench-to-bedside review: endotoxin tolerance as a model of leukocyte reprogramming in sepsis. *Crit Care*. 2006;10(5):233.

18. Pena OM, et al. An endotoxin tolerance signature predicts sepsis and organ dysfunction at initial clinical presentation. *EBioMedicine*. 2014;1(1):64–71.

19. Shalova IN, et al. Human monocytes undergo functional re-programming during sepsis mediated by hypoxia-inducible factor-1α. *Immunity*. 2015;42(3):484–498.

20. Angus DC, van der Poll T. Severe sepsis and septic shock. *N Engl J Med*. 2013;369(9):840–851.

21. Escoll P, et al. Rapid up-regulation of IRAK-M expression following a second endotoxin challenge in human monocytes and in monocytes isolated from septic patients. *Biochem Biophys Res Commun*. 2003;311(2):465–472.

22. Biswas SK, Lopez-Collazo E. Endotoxin tolerance: new mechanisms, molecules and clinical significance. *Trends Immunol*. 2009;30(10):475–487.

23. López-Collazo E, del Fresno C. Pathophysiology of endotoxin tolerance: mechanisms and clinical consequences. *Crit Care*. 2013;17(6):242.

24. Ariga SK, et al. Endotoxin tolerance drives neutrophil to infectious site. *Shock*. 2014;42(2):168–173.

25. Berg DJ, et al. Interleukin-10 is a central regulator of the response to LPS in murine models of endotoxic shock and the Shwartzman reaction but not endotoxin tolerance. *J Clin Invest*. 1995;96(5):2339–2347.

26. Wysocka M, et al. IL-12 suppression during experimental endotoxin tolerance: dendritic cell loss and macrophage hyporesponsiveness. *J Immunol*. 2001;166(12):7504–7513.

27. Kobayashi K, Hernandez LD, Galán JE, Janeway CA, Medzhitov R, Flavell RA. IRAK-M is a negative regulator of Toll-like receptor signaling. *Cell*. 2002;110(2):191–202.

28. Sly LM, Rauh MJ, Kalesnikoff J, Song CH, Krystal G. LPS-induced upregulation of SHIP is essential for endotoxin tolerance. *Immunity*. 2004;21(2):227–239.

29. Xiong Y, Medvedev AE. Induction of endotoxin tolerance in vivo inhibits activation of IRAK4 and increases negative regulators IRAK-M, SHIP-1, and A20. *J Leukoc Biol*. 2011;90(6):1141–1148.

30. Ziegler-Heitbrock L. The p50-homodimer mechanism in tolerance to LPS. *J Endotoxin Res*. 2001;7(3):219–222.

31. Adib-Conquy M, et al. NF-κB expression in mononuclear cells of patients with sepsis resembles that observed in lipopolysaccharide tolerance. *Am J Respir Crit Care Med*. 2000;162(5):1877–1883.

32. Carmody RJ, Chen YH. Nuclear factor-κB: activation and regulation during Toll-like receptor signaling. *Cell Mol Immunol*. 2007;4(1):31–41.

33. Hayden MS, Ghosh S. Shared principles in NF-κB signaling. *Cell*. 2008;132(3):344–362.

34. Biswas SK, Tergaonkar V. Myeloid differentiation factor 88-independent Toll-like receptor pathway: sustaining inflammation or promoting tolerance? *Int J Biochem Cell Biol*. 2007;39(9):1582–1592.

35. Toshchakov V, et al. TLR4, but not TLR2, mediates IFN-β-induced STAT1α/β-dependent gene expression in macrophages. *Nat Immunol*. 2002;3(4):392–398.

36. Akira S, Takeda K. Toll-like receptor signalling. *Nat Rev Immunol*. 2004;4(7):499–511.

37. Dejager L, et al. Pharmacological inhibition of type I interferon signaling protects mice against lethal sepsis. *J Infect Dis*. 2014;209(6):960–970.

38. Harper JW, Adami GR, Wei N, Keyomarsi K, Elledge SJ. The p21 Cdk-interacting protein Cip1 is a potent inhibitor of G1 cyclin-dependent kinases. *Cell*. 1993;75(4):805–816.

39. Balomenos D, et al. The cell cycle inhibitor p21 controls T-cell proliferation and sex-linked lupus development. *Nat Med*. 2000;6(2):171–176.

40. Salvador JM, et al. Mice lacking the p53-effector gene Gadd45a develop a lupus-like syndrome. *Immunity*. 2002;16(4):499–508.

41. Zhu B, et al. Early growth response gene 2 (Egr-2) controls the self-tolerance of T cells and prevents the development of lupuslike autoimmune disease. *J Exp Med*. 2008;205(10):2295–2307.

42. Chen H, et al. CD4+ T cells from elite controllers resist HIV-1 infection by selective upregulation of p21. *J Clin Invest*. 2011;121(4):1549–1560.

43. Lloberas J, Celada A. p21(waf1/CIP1), a CDK inhibitor and a negative feedback system that controls macrophage activation. *Eur J Immunol*. 2009;39(3):691–694.

44. Arias CF, et al. p21CIP1/WAF1 controls proliferation of activated/memory T cells and affects homeostasis and memory T cell responses. *J Immunol*. 2007;178(4):2296–2306.

45. Daszkiewicz L, et al. Distinct p21 requirements for regulating normal and self-reactive T cells through IFN-γ production. *Sci Rep*. 2015;5:7691.

46. Trakala M, et al. Regulation of macrophage activation and septic shock susceptibility via p21(WAF1/CIP1). *Eur J Immunol*. 2009;39(3):810–819.

47. Scatizzi JC, et al. The CDK domain of p21 is a suppressor of IL-1β-mediated inflammation in activated macrophages. *Eur J Immunol*. 2009;39(3):820–825.

48. Mavers M, et al. Cyclin-dependent kinase inhibitor p21, via its C-terminal domain, is essential for resolution of murine inflammatory arthritis. *Arthritis Rheum*. 2012;64(1):141–152.

49. Ghosn EE, et al. Two physically, function-

ally, and developmentally distinct peritoneal macrophage subsets. *Proc Natl Acad Sci U S A.* 2010;107(6):2568–2573.

50. Ní Gabhann J, et al. Btk regulates macrophage polarization in response to lipopolysaccharide. *PLoS One.* 2014;9(1):e85834.

51. Singh P, et al. DUSP3 Genetic deletion confers M2-like macrophage-dependent tolerance to septic shock. *J Immunol.* 2015;194(10):4951–4962.

52. Groeneveld PH, Claassen E, Kuper CF, Van Rooijen N. The role of macrophages in LPS-induced lethality and tissue injury. *Immunology.* 1988;63(3):521–527.

53. Trinchieri G. Type I interferon: friend or foe? *J Exp Med.* 2010;207(10):2053–2063.

54. Swiecki M, Colonna M. The multifaceted biology of plasmacytoid dendritic cells. *Nat Rev Immunol.* 2015;15(8):471–485.

55. Nakano H, Yanagita M, Gunn MD. CD11c(+) B220(+)Gr-1(+) cells in mouse lymph nodes and spleen display characteristics of plasmacytoid dendritic cells. *J Exp Med.* 2001;194(8):1171–1178.

56. McDunn JE, et al. Splenic CD4⁺ T cells have a distinct transcriptional response six hours after the onset of sepsis. *J Am Coll Surg.* 2006;203(3):365–375.

57. de Pablo R, Monserrat J, Prieto A, Alvarez-Mon M. Role of circulating lymphocytes in patients with sepsis. *Biomed Res Int.* 2014;2014:671087.

58. Aird WC. The role of the endothelium in severe sepsis and multiple organ dysfunction syndrome. *Blood.* 2003;101(10):3765–3777.

59. Lush CW, Cepinskas G, Kvietys PR. LPS tolerance in human endothelial cells: reduced PMN adhesion, E-selectin expression, and NF-κB mobilization. *Am J Physiol Heart Circ Physiol.* 2000;278(3):H853–H861.

60. Biswas SK, et al. Role for MyD88-independent, TRIF pathway in lipid A/TLR4-induced endotoxin tolerance. *J Immunol.* 2007;179(6):4083–4092.

61. Kawai T, Akira S. Signaling to NF-κB by Toll-like receptors. *Trends Mol Med.* 2007;13(11):460–469.

62. Garoufalis E, et al. Viral induction of the human β interferon promoter: modulation of transcription by NF-κB/rel proteins and interferon regulatory factors. *J Virol.* 1994;68(8):4707–4715.

63. Frankenberger M, Ziegler-Heitbrock HW. LPS tolerance in monocytes/macrophages: three 3′ cytosins are required in the DNA binding motif

for detection of upregulated NF-κB p50 homodimers. *Immunobiology.* 1997;198(1–3):81–90.

64. Carmody RJ, Ruan Q, Palmer S, Hilliard B, Chen YH. Negative regulation of Toll-like receptor signaling by NF-κB p50 ubiquitination blockade. *Science.* 2007;317(5838):675–678.

65. Guan H, Hou S, Ricciardi RP. DNA binding of repressor nuclear factor-κB p50/p50 depends on phosphorylation of Ser 337 by the protein kinase A catalytic subunit. *Biochemistry.* 2005;280(11):9957–9962.

66. Faas MM, et al. Monocyte intracellular cytokine production during human endotoxaemia with or without a second in vitro LPS challenge: effect of RWJ-67657, a p38 MAP-kinase inhibitor, on LPS-hyporesponsiveness. *Clin Exp Immunol.* 2002;127(2):337–343.

67. Fernández-Ruiz I, et al. Mitochondrial DAMPs induce endotoxin tolerance in human monocytes: an observation in patients with myocardial infarction. *PLoS One.* 2014;9(5):e95073.

68. del Fresno C, et al. Monocytes from cystic fibrosis patients are locked in an LPS tolerance state: down-regulation of TREM-1 as putative underlying mechanism. *PLoS One.* 2008;3(7):e2667.

69. Merched AJ, Chan L. Absence of p21Waf1/Cip1/Sdi1 modulates macrophage differentiation and inflammatory response and protects against atherosclerosis. *Circulation.* 2004;110(25):3830–3841.

70. Rajaiah R, Perkins DJ, Polumuri SK, Zhao A, Keegan AD, Vogel SN. Dissociation of endotoxin tolerance and differentiation of alternatively activated macrophages. *J Immunol.* 2013;190(9):4763–4772.

71. Liew FY, Xu D, Brint EK, O'Neill LA. Negative regulation of Toll-like receptor-mediated immune responses. *Nat Rev Immunol.* 2005;5(6):446–458.

72. Del Fresno C, et al. Potent phagocytic activity with impaired antigen presentation identifying lipopolysaccharide-tolerant human monocytes: demonstration in isolated monocytes from cystic fibrosis patients. *J Immunol.* 2009;182(10):6494–6507.

73. van 't Veer C, et al. Induction of IRAK-M is associated with lipopolysaccharide tolerance in a human endotoxemia model. *J Immunol.* 2007;179(10):7110–7120.

74. Seok J, et al. Genomic responses in mouse models poorly mimic human inflammatory diseases. *Proc Natl Acad Sci U S A.* 2013;110(9):3507–3512.

75. McNab F, Mayer-Barber K, Sher A, Wack A, O'Garra A. Type I interferons in infectious disease. *Nat Rev Immunol.* 2015;15(2):87–103.

76. Yoo CH, Yeom JH, Heo JJ, Song EK, Lee SI, Han MK. Interferon β protects against lethal endotoxic and septic shock through SIRT1 upregulation. *Sci Rep.* 2014;4:4220.

77. Karaghiosoff M, et al. Central role for type I interferons and Tyk2 in lipopolysaccharide-induced endotoxin shock. *Nat Immunol.* 2003;4(5):471–477.

78. Huys L, et al. Type I interferon drives tumor necrosis factor-induced lethal shock. *J Exp Med.* 2009;206(9):1873–1882.

79. Mahieu T, et al. The wild-derived inbred mouse strain SPRET/Ei is resistant to LPS and defective in IFN-β production. *Proc Natl Acad Sci U S A.* 2006;103(7):2292–2297.

80. Mahieu T, Libert C. Should we inhibit type I interferons in sepsis? *Infect Immun.* 2007;75(1):22–29.

81. Bohuslav J, et al. Regulation of an essential innate immune response by the p50 subunit of NF-κB. *J Clin Invest.* 1998;102(9):1645–1652.

82. Wessells J, et al. BCL-3 and NF-κB p50 attenuate lipopolysaccharide-induced inflammatory responses in macrophages. *J Biol Chem.* 2004;279(48):49995–50003.

83. Kuwata H, et al. IL-10-inducible Bcl-3 negatively regulates LPS-induced TNF-α production in macrophages. *Blood.* 2003;102(12):4123–4129.

84. Rousselle A, et al. CXCL5 limits macrophage foam cell formation in atherosclerosis. *J Clin Invest.* 2013;123(3):1343–1347.

85. Mantovani A, Garlanda C, Locati M. Macrophage diversity and polarization in atherosclerosis: a question of balance. *Arterioscler Thromb Vasc Biol.* 2009;29(10):1419–1423.

86. Moore KJ, Sheedy FJ, Fisher EA. Macrophages in atherosclerosis: a dynamic balance. *Nat Rev Immunol.* 2013;13(10):709–721.

87. [No authors listed]. American College of Chest Physicians/Society of Critical Care Medicine Consensus Conference: definitions for sepsis and organ failure and guidelines for the use of innovative therapies in sepsis. *Crit Care Med.* 1992;20(6):864–874.